

HIGH-PERFORMANCE COMPUTING: APPLICATION TO AB-INITIO SIMULATIONS OF X-RAY ABSORPTION SPECTRA FROM NANOPARTICLES

A. Kuzmin

Institute of Solid State Physics, University of Latvia, Kengaraga Street 8, LV-1063 Riga, Latvia
e-mail: a.kuzmin@cfi.lu.lv, fax: +371 7132778, phone: +371 7251691

ABSTRACT

This paper discusses basics of high performance computing on the example of the Latvian SuperCluster (LASC), installed at the Institute of Solid State Physics of the University of Latvia. The application of LASC to ab-initio simulations of x-ray absorption spectra from nanoparticles is considered as a particular case.

[Keywords: *high performance computing, cluster computing, x-ray absorption spectroscopy, nanoparticles*]

INTRODUCTION

High-performance computing (HPC) is associated with the use of high-end computer systems, so-called 'supercomputers', for solving complicated computational problems. Today HPC infrastructure is a critical resource for research and development as well as for many business applications. The standard tasks, which are addressed by HPC systems, require normally hundreds or even thousands of processor hours to complete. Therefore special approaches, based on dedicated software and hardware components, have to be used.

The first HPC systems have appeared in the late 1970s, when the Cray-1 and CDC Cyber 203/205 supercomputers were built. The computation speed of the Cray-1 system was about 160 MFlops, it was equipped with an 8 megabyte main memory and priced \$8.8 million [1]. A tremendous progress in the HPC field during past decades resulted in supercomputers speedup more than five orders of magnitude. By the end of 2002, the most powerful existing HPC systems had performance in the range from 3 to 36 TFlops. The top five supercomputers include Earth-Simulator (35.86 TFlops, 5120 processors), installed by NEC in 2002 [2]; two ASCI Q systems (7.72 TFlops, 4096 processors), built by Hewlett-Packard in 2002 and based on the AlphaServer SC computer systems [3]; ASCI White (7.23 TFlops, 8192 processors), installed by IBM in 2000 [3]; and, a pleasant surprise, MCR Linux Cluster (5.69 TFlops, 2304 Xeon 2.4 GHz processors), built by Linux NetworX in 2002 for Lawrence Livermore National Laboratory (USA) [4].

An increase of performance of HPC systems is connected with the progress in their architectures [5]. Whereas the first supercomputers as Cray-1 were based on vector technology with shared-memory architecture (Figure 1(a)), the massive parallel processing (MPP) systems using distributed-memory (Figure 1(b)), were introduced by the end of the 1980s.

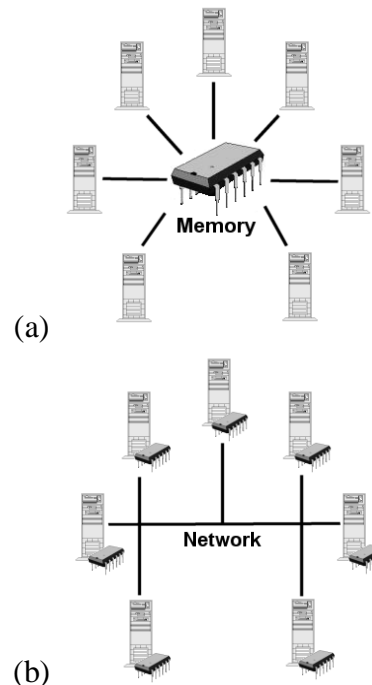


FIGURE 1. SHARED (A) AND DISTRIBUTED (B) MEMORY COMPUTER ARCHITECTURES.

Conventional MPP supercomputers are oriented on the highest level of performance that makes them expensive and requires special maintenance support. Therefore, to meet the requirements of the lower and medium market segments, the symmetric multiprocessing (SMP) systems were introduced in the early 1990s to address commercial users with applications such as databases, scheduling tasks in telecommunications industry, data mining and manufacturing.

Recently, a significant improvement in the communication network technologies and standard workstation processors speed as well as better understanding of applications and algorithms led to emerging of new class of systems, called *clusters of SMP* or *networks of workstations* (NOW). Cluster based systems are able to compete in performance with MPPs and have excellent price/performance ratios for special applications types. According to the recent TOP500 Supercomputers List from November 2002 [6], cluster based systems represent 18.6% from all supercomputers, and most of them (about 60%) use Intel's processors. In principle, clustering technology can be implemented for any arbitrary group of computers, allowing

to build homogeneous or heterogeneous systems. Even bigger performance can be gained by combining groups of clusters into HyperCluster or even Grid-type system [7].

In this paper we will discuss the basics of cluster HPC on the example of the Latvian SuperCluster (LASC) project. An example of the LASC application to the physical problem - ab-initio simulations of x-ray absorption spectra from nanoparticles - will be also considered.

HIGH-PERFORMANCE COMPUTING

Basics of cluster computing

Cluster computing refers to technologies that allow multiple computers, called cluster nodes, to work together with the aim to solve common computing problems. A generic cluster architecture is shown in Figure 2. Each node can be a single or multiprocessor computer, such as a PC, workstation or SMP server, equipped with its own memory, I/O devices and operating system. The cluster, having similar nodes, is called homogeneous, otherwise - heterogeneous. The nodes are usually interconnected by local area network (LAN) based on one of the following technologies [5]: Ethernet, Fast Ethernet, Gigabit Ethernet, Myrinet, Quadrics Network (QsNet), InfiniBand communication fabric, Scalable Coherent Interface (SCI), Virtual Interface Architecture (VIA) or Memory Channel. The optimal choice of the network type is dictated by demands on speed and volume of data exchange between several parts of the application software, running on different nodes. The nodes in the cluster are managed by Linux, Solaris and Windows operating systems. However, in order for the cluster to be able to pool its computing resources, special cluster-enabled applications must be written using clustering libraries or a system level *middleware* [8] should be used. The most popular clustering libraries are PVM (Parallel Virtual Machine) [9] and MPI (Message Passing Interface) [10]. By using PVM or MPI, programmers can design applications that can span across an entire cluster's computing resources rather than being confined to the resources of a single machine. For many applications, PVM and MPI allow computing problems to be solved at a rate that scales almost linearly in relation to the number of processors in the cluster.

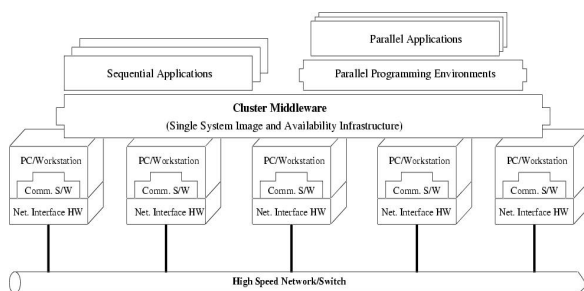


FIGURE 2. TYPICAL CLUSTER ARCHITECTURE [11].

The cluster architecture is usually optimised for *High Performance Computing* or *High Availability Computing*. The choice of the architecture is dictated by the type of an application and available budget. A combination of both approaches is utilised in some cases, resulting in a highly reliable system, characterized by a very high performance.

The principal difference between these two approaches consists of that in the HPC case, each node in the cluster executes a part of the common job, whereas in the second case, several nodes perform or are ready to perform the same job and, thus, are able to substitute each other in a case of failure.

High availability (HA) clusters are normally used in mission critical applications to have constant availability of services to end-users through multiple instances of one or more applications on many computing nodes. Such systems found their application as Web servers, e-commerce engines or database servers.

HPC clusters are built to improve processing throughput in order to handle multiple jobs of various sizes and types or to increase performance. The most common HPC clusters are used to shorten turnaround times on compute-intensive problems by running the job on multiple nodes at the same time or when the problem is just too big for a single system. This is often the case in scientific, design analysis and research computing, where the HPC cluster is built purely to obtain maximum performance during the solution of a single, very large problem. Such HPC clusters utilise parallelised software that breaks down the problem into smaller parts, which are dispatched across a network of interconnected systems that concurrently process each small part and then communicate with each other using message-passing libraries to coordinate and synchronize their results. The Beowulf-type cluster [12], which will be described in the next section, is an example of the HPC system. Beowulf system is the cluster which is built primarily out of commodity hardware components, is running a free-software operating system like Linux or FreeBSD and is interconnected by a private high-speed network. However, some Linux clusters, which are built for high availability instead of speed, are not Beowulfs.

Latvian SuperCluster (LASC)

In this section we will describe the Beowulf-type cluster - the Latvian SuperCluster (LASC) [13], installed at the Institute of Solid State Physics of the University of Latvia in 2002.

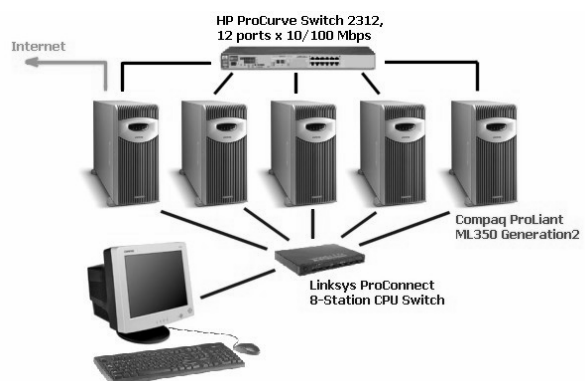


FIGURE 3. LATVIAN SUPERCLUSTER (LASC) STRUCTURE.

At present, the LASC (Figure 3) consists of five nodes: one front-end node plus four computational nodes. The nodes, Compaq ProLiant ML350 G2 servers, are interconnected through Fast Ethernet switch, and the front-end node has also a connection with the rest of the world

(Internet). The total resources available to the users are 10 Pentium III-1.26GHz CPUs, having a total peak power about 13 GFlops, 20 GB of physical memory (RAM) and 456 GB of storage space on UATA-100 IDE/SCSI hard disks (easily expandable up to 3.3 TB).

The nodes are running under the Red Hat Linux operating system on the private subnetwork, protected from the Internet by a firewall. Most of installed software is of open source type and, thus, is available for free under GNU public license. The cluster security is maintained through the use of secure shell interface (SSH2) and client's authorisation by the IP address. For users convenience, all information related to the cluster is available on-line from the Web service [13].

The storage disks space in the cluster is shared among all the nodes via Network File System (NFS), so that all data as well as home directories of the users are accessible on all nodes in a similar way. As on any UNIX system, the users applications can run in interactive mode, in background mode or in batch mode. At present time, to launch an application on the particular node, the user should login to that node first or use an automatic job submitting system, called CLRUN. The CLRUN system allows (i) to submit a job from any node to any node for execution and (ii) to display the load for every node and all user's processes on each nodes. In the future, we plan to install openMOSIX load balancing system to improve the overall cluster performance and to simplify its use. The programming environment available to the users consists of the GNU set of compilers (C/C++/Fortran/Pascal) and the Intel's C++/Fortran compilers, which have better degree of optimization and able to automatically parallelise a user's code on SMP systems. To use the entire cluster's computing resources within user's applications, the popular clustering libraries such as PVM and MPI are available.

The LASC system represents a classical example of the "home-made" Beowulf-type cluster. Currently, its main use is dedicated to quantum chemistry calculations, Monte-Carlo modelling and x-ray absorption spectra simulations. Similar systems can be easily build up for other than scientific needs with possibly even lower price. As an example, standard "off-the-shelf" computers, equipped with much smaller memory and thus being much cheaper, can be used as nodes in a cluster for multimedia encoding applications, such as sound MPEG-3 or video MPEG-4 processing, and for images rendering to create stunning three-dimensional graphics.

AB-INITIO SIMULATIONS OF X-RAY ABSORPTION SPECTRA FROM NANOPARTICLES

Introduction to x-ray absorption spectroscopy

Development of advanced materials with controlled properties requires precise knowledge of their atomic structure. Two direct structural techniques are currently available: x-ray/neutron scattering and x-ray absorption spectroscopy (XAS). While the first method is well known and was widely used for many decades, XAS is relatively new and comes into the force during the last 10-15 years [14]. The success of XAS is connected with an appearance of synchrotron radiation sources, which produce x-rays with the intensity being 10-to-16 orders of magnitude higher than from conventional x-ray tubes.

XAS is a local tool that makes it applicable to a study of any material from molecules to single-crystals [14]. It provides with a complementary to other techniques information on the short-range order (SRO) around an absorbing atom and has several advantages. In fact, XAS is more sensitive to the variations of the SRO than x-ray or neutron scattering, especially, in the case of disordered or multicomponent compounds, such as alloys, glasses, mixed crystals, liquids, etc. In such complex materials, the strong advantage of XAS is connected with the possibility to probe the local environment of the same type atoms independently

Besides, XAS is successfully applied for in situ studies of phase transitions and chemical reactions due to possibility to work with small amount of material and to perform very fast measurements (order of milliseconds). Finally, XAS is also sensitive to the local density of empty electron states at the absorber, thus providing with unique information on the antibonding or conduction band states.

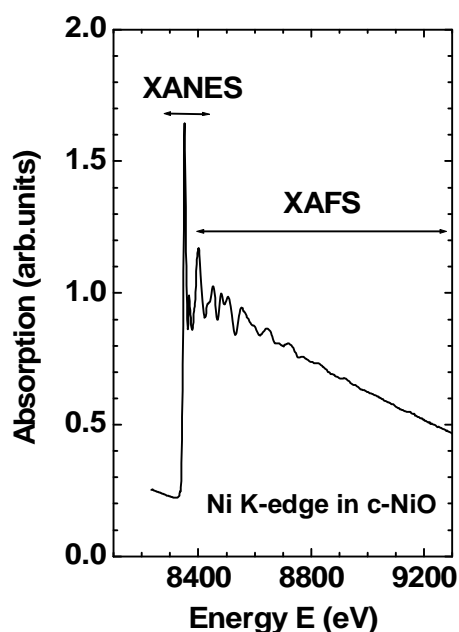


FIGURE 4. NI K-EDGE X-RAY ABSORPTION SPECTRUM IN CRYSTALLINE NiO [14].

The information on the SRO (atom types, coordination numbers, interatomic distances and mean square relative displacements (MSRD) of atoms) around the absorbing atom is contained within the x-ray absorption fine structure (XAFS), which is located beyond the absorption edge of an atom (Figure 4). The XAFS range extends usually about 400-1000 eV above the edge and is limited by experimental noise and/or by the presence of another absorption edge. Modern approach to the analysis of the XAFS spectra has been developed in the 1990s [15,16] and requires an intensive use of modern computers. It allows rather precise calculation of the XAFS spectrum for the frozen configuration of atoms, however ab-initio treatment of thermal vibrations and static disorder is still among unresolved questions. The main problem is caused by the difficulties in the calculation of correlations in atomic motion for n-atoms configurations and the inclusion of such effects into the XAFS formalism. The easiest way to address these problems is to use Molecular Dynamics or Monte-Carlo approaches, which allow to work with the

configuration averages instead of the time averages. Such approach follows closely the real experimental situation, because the characteristic time of the x-ray absorption event is only $\sim 10^{-16}$ seconds, whereas the characteristic time of atomic vibrations is $\sim 10^{-13} \div 10^{-14}$ seconds. Therefore, measured experimentally x-ray absorption spectrum is an average over many snapshots of frozen atomic configurations.

Ab-Initio Calculation of XAFS

The XAFS signal for a frozen configuration of atoms can be calculated according to the diagram in Figure 5. The full procedure can be separated into four main steps [15]: (1) calculation of the cluster potential as a sum of overlapped muffin-tin spherical potentials; (2) calculation of embedded-atomic cross-section and partial wave phase shifts; (3) finding of x-ray absorption near edge structure (XANES) within full-multiple scattering (FMS) formalism or of XAFS within multiple scattering (MS) approach; (4) calculation of the total absorption coefficient/absorption cross-section. In this procedure, the first and the third steps are the most time consuming. Note that opposite to conventional electronic structure calculations, the XAFS calculations involve the use of complex energy dependent exchange-correlation potential (ECP). This allows to account for inelastic losses of the excited photoelectron in extrinsic channels on plasmon excitations. In this work the complex Hedin-Lundqvist ECP [15], based on the density functional formalism within the single-plasmon pole approximation, was used. The final state of absorbing nickel atoms was taken to be fully relaxed with a hole localized in the 1s(Ni) core site.

The calculation of the cluster potential, based on the self-consistent procedure, requires normally few hours of 1 GFLOP CPU time for a cluster of several tens atoms. Fortunately, due to small sensitivity of the excited electron, having large kinetic energy, to small variations of the cluster potential, this step can be performed, in most cases, just once for an average configuration of atoms. Thus, the simulation of XANES and/or XAFS signals remains the main problem.

The XANES calculations within FMS formalism require an inversion of the large $(1-tG^0)$ matrix (Figure 5) that makes them very time consuming. It can take up to 1-2 days of 1 GFLOP CPU time for a cluster of several hundreds atoms. At the same time, the total XAFS signal for such cluster can be calculated within several tens seconds that makes the job practically feasible.

Further we will discuss an example of XAFS simulations for nickel oxide nanoparticles using the Monte-Carlo method.

Nickel Oxide Nanoparticles Model

The model represents spherical particle, consisting of nickel and oxygen atoms ordered on slightly distorted rock-salt-type lattice with the lattice parameter $a = 4.1773 \text{ \AA}$ as in bulk NiO [17]. The distortion appears as random displacements of nickel and oxygen atoms from regular lattice sites and approximates thermal disorder present in the real material. The amount of displacements was estimated from atoms thermal ellipsoids, determined by the Rietveld-type analysis of x-ray powder diffraction patterns in [18].

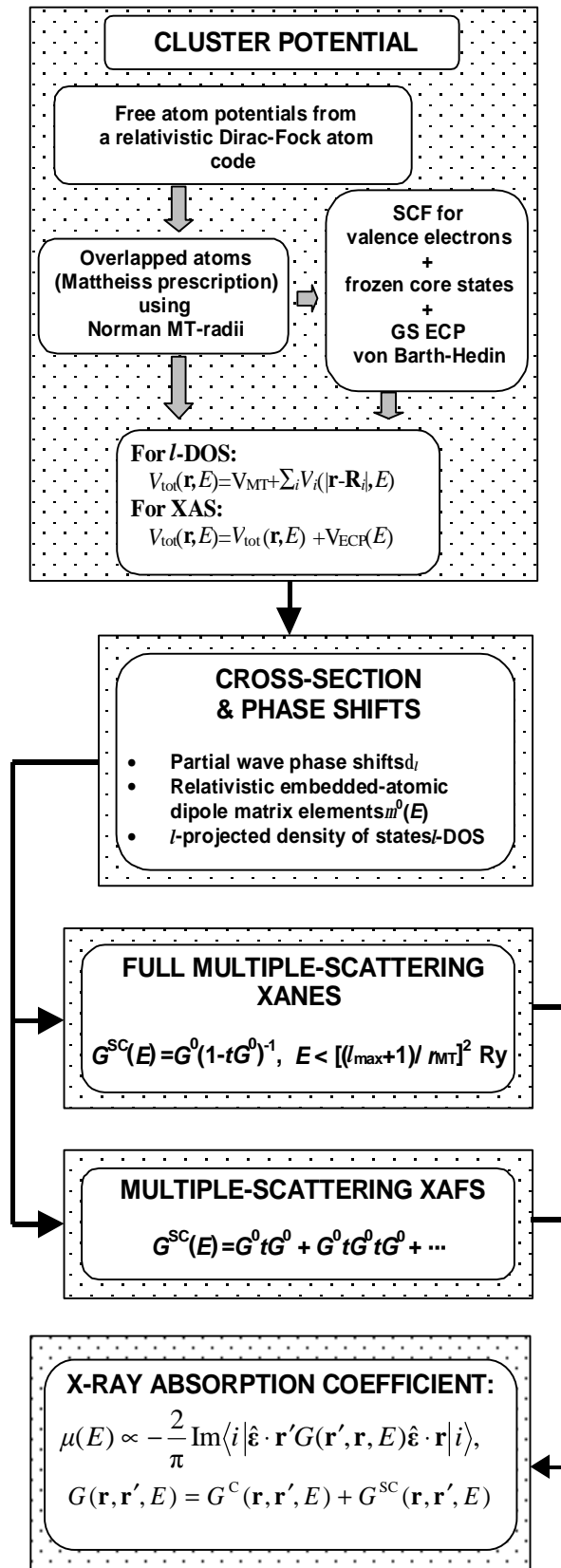


FIGURE 5. DIAGRAM OF AB INITIO SELF-CONSISTENT REAL SPACE MULTIPLE-SCATTERING CALCULATION OF X-RAY ABSORPTION SPECTRUM WITHIN THE GREEN'S FUNCTION FORMALISM.

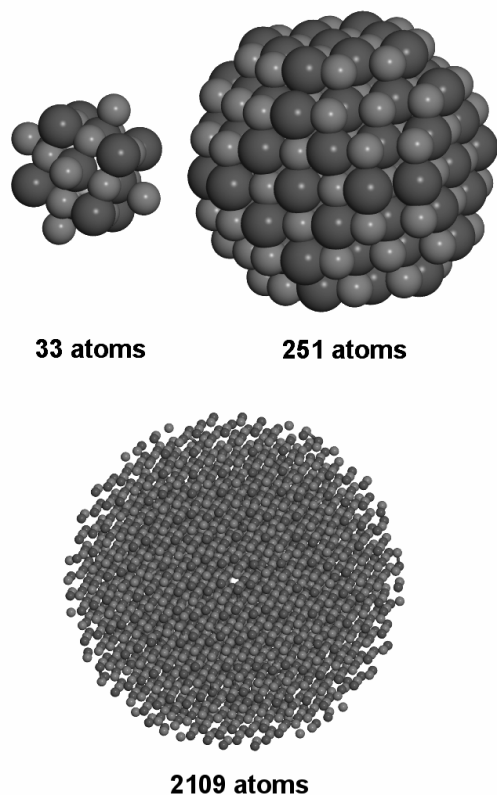


FIGURE 6. EXAMPLE OF NiO NANOPARTICLES MODELS: 33 ATOMS ($D=8.4 \text{ \AA}$), 251 ATOMS ($D=16.7 \text{ \AA}$) AND 2109 ATOMS ($D=33.4 \text{ \AA}$). OXYGEN ATOMS ARE LARGE DARK-GRAY, NICKEL ATOMS ARE SMALL LIGHT-GRAY.

Thus, the only varied parameter in our model is the size (diameter) of the particle.

Several particles of different sizes were constructed (Figure 6). The size was varied from 8.4 to 83.5 Å that corresponds to particles composed of 33 to 33401 atoms. The change in the particle size influences the ratio of surface-to-bulk atoms. As a result, a decrease of the particle size leads to larger reduction of the average coordination number for more distant shells. This effect can be readily observed in the Ni K-edge XAFS spectra.

Ab-Initio Calculations of X-Ray Absorption Spectra for Nickel Oxide Nanoparticles

Bulk nickel oxide has the rock-salt type structure [17,18]. When prepared as thin film, e.g. by reactive dc magnetron sputtering [19], nickel oxide has nanocrystalline structure. Previous results, based on rather rough model, have suggested the average crystallites size to be about 21-34 Å [19]. The structure of these nano-sized crystallites resembles closely the one of c-NiO with some exceptions: the lattice parameter for freshly prepared thin films is about 0.05 Å larger than that of crystalline material, and a relaxation of the first nickel coordination shell, composed of six oxygen atoms, occurs in the films leading to the shortening of the average Ni-O distance [19].

The experimental XAFS signals $\chi(k)k^2$ and their Fourier transforms (FTs) for bulk NiO and two thin films, sputtered in mixed Ar+O₂ atmosphere with different oxygen content,

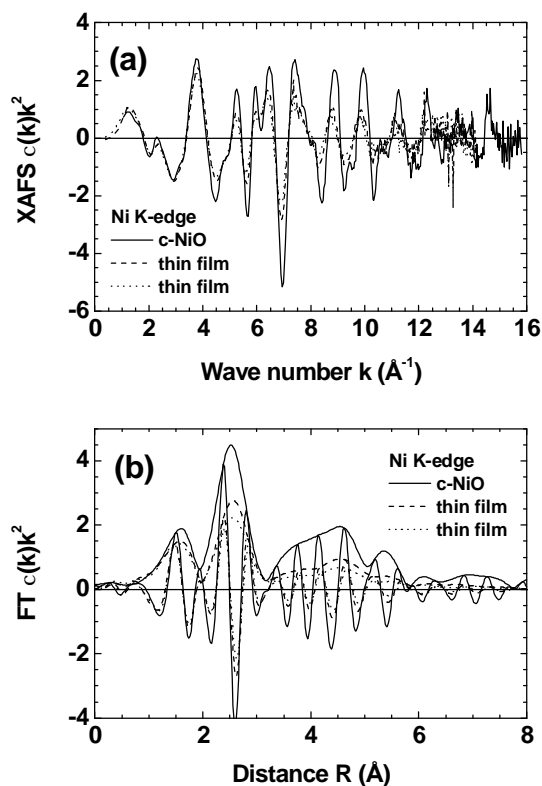


FIGURE 7. EXPERIMENTAL XAFS $\chi(k)k^2$ SIGNALS (a) AND THEIR FOURIER TRANSFORMS (b) FOR BULK c-NiO AND NANOCRYSTALLINE NICKEL OXIDE THIN FILMS [19].

are shown in Figure 7. The FT of the XAFS signal looks like a pair distribution function, however it is not [14]: the shape and position of peaks in FT are strongly affected by the atomic scattering amplitudes and phase shifts, besides, the multiple-scattering contributions, i.e. XAFS signals from high-order distribution functions, result in additional peaks, located at positions which do not correspond to the coordination shells radii.

The experimental data in Figure 7 show clearly that the effect of crystallinity affects mainly the amplitude of XAFS signal, whereas the phase remains nearly unchanged. This behaviour is typical for nanocrystalline compounds. The effects of lattice expansion and local structure relaxation around nickel atoms, observed in previous work [19], are both much smaller and, therefore, were neglected in our simulations.

For each nickel oxide nanoparticle (Figure 6), the total XAFS $\chi_{total}(k)$ signal can be determined by averaging over all nickel atoms:

$$C_{total}(k) = \frac{1}{n} \sum_{i=1}^n C_i(k),$$

where n is the total number of nickel atoms. Since the experimental data give the radial information till about 8 Å (Figure 7(b)) around nickel atoms, it is possible to speed-up the calculation of $\chi_{total}(k)$ by dividing the spherical nanoparticle into two regions: (i) the *bulk* region, containing all atoms close to the center inside the sphere with the radius

by 8 Å smaller than the radius of the nanoparticle itself and (ii) the *surface* region, containing all remaining atoms located within the 8 Å layer near the surface. Besides, our estimates suggest that in the case of similar enough environment, an average over about hundred XAFS spectra is sufficient to get good approximation to the total XAFS spectrum. Therefore an amount of calculations within the bulk region can be significantly reduced because the local environment of all nickel atoms is close and differ only due to thermal disorder. Thus, the total XAFS signal in our simulation is given by

$$c_{total}(k) = \frac{1}{m} \sum_{i=1}^m c_i^{surface}(k) + \frac{1}{100} \sum_{i=1}^{100} c_i^{bulk}(k),$$

where the terms are due to averaging over nickel atoms in the surface and bulk regions. The calculation time was ranging between about 8 minutes for the smallest nanoparticle with the diameter 8.4 Å to about 34 hours for the largest one having the diameter 83.5 Å.

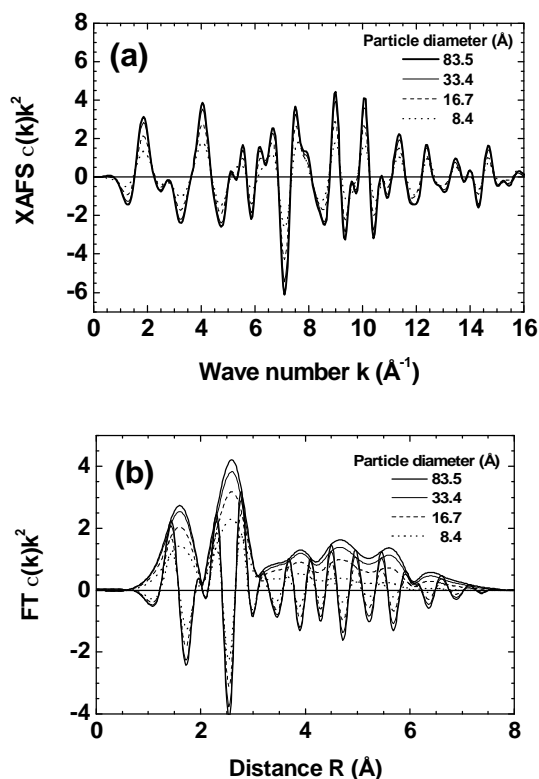


FIGURE 8. CALCULATED Ni K-EDGE XAFS $\chi(k)k^2$ SIGNALS (a) AND THEIR FOURIER TRANSFORMS (b) FOR NANOPARTICLES WITH DIFFERENT SIZE.

The obtained results for several nanoparticles are shown in Figure 8. They follow well the tendencies found for experimental XAFS signals: a decrease of the particle size results in the progressive reduction of the outer shells amplitude. The amount of reduction is significant for nanoparticles with a size less than about 50 Å that limits the range of size sensitivity in this case. The XAFS signal corresponding to the nanoparticle with the diameter 83.5 Å is nearly undistinguishable from that for the bulk. By comparing the Figures 7 and 8, one can conclude that nanoparticles in the thin films have the diameter of about 10

Å and are composed of about 60 atoms. This size is of the same order of magnitude as estimated previously in [19].

CONCLUSIONS

The use of cluster HPC system, the Latvian SuperCluster [13], allowed us to perform ab-initio modelling of the XAFS spectra of nanocrystalline nickel oxide thin films and to estimate the size of nanocrystallites. Similar approach can be used for other nanosized materials.

ACKNOWLEDGEMENT

This work was supported in part by the Latvian Government Research Grants No. 01.0807 and 01.0821. The author wish to thank all colleagues from the ISSP UL for support of the LASC project.

REFERENCES

- [1] <http://www.cray.com/>
- [2] <http://www.es.jamstec.go.jp/>
- [3] <http://www.llnl.gov/asci/platforms/>
- [4] <http://www.llnl.gov/linux/mcr/>
- [5] Kuzmin A. (2003) Cluster approach to high performance computing. *Computer Modelling and New Technologies* (in press).
- [6] <http://www.top500.org/>
- [7] <http://www.gridcomputingplanet.com/>
- [8] <http://www.cs.wisc.edu/condor/>
- [9] http://www.epm.ornl.gov/pvm/pvm_home.html
- [10] <http://www-unix.mcs.anl.gov/mpi/>
- [11] Buyya R. (ed.) (1999) *High Performance Cluster Computing: Systems and Architectures*. Prentice Hall, New York.
- [12] <http://www.beowulf.org/>
- [13] <http://www.cfi.lu.lv/lasc>
- [14] Aksenov V.L., Kuzmin A.Y., Purans J., and Tyutyunnikov S.I. (2001) EXAFS Spectroscopy at Synchrotron-Radiation Beams. *Phys. Part. Nucl.* **32** 675-707.
- [15] Ankudinov A.L., Ravel B., Rehr J.J., and Conradson S.D. (1998) Real-space multiple-scattering calculation and interpretation of x-ray-absorption near-edge structure. *Phys. Rev. B* **58**, 7565-7576.
- [16] Filipponi A, Di Cicco A, Tyson T.A., and Natoli C.R. (1991) *Ab-initio modelling of x-ray absorption spectra. Solid State Commun.* **78**, 265-268.
- [17] Kuzmin A. and Mironova N. (1998) Composition dependence of the lattice parameter in Ni_cMg_{1-c}O solid solutions. *J. Phys.: Condensed Matter* **10**, 7937-7944.
- [18] Massarotti V., Capsoni D., Berbenni V., Riccardi R., Marini A., and Antolini E. (1991) Structural characterization of nickel oxide. *Z. Naturforsch. A* **46**, 503-512.
- [19] Kuzmin A., Purans J., and Rodionov A. (1997) X-ray absorption spectroscopy study of the Ni K-edge in magnetron sputtered nickel oxide thin films. *J. Phys.: Condensed Matter* **9**, 6979-6993.